



Numerical simulation of ceramic breeder pebble bed thermal creep behavior

Alice Ying^{*}, Hulin Huang, Mohamed Abdou

Mechanical and Aerospace Engineering Department, UCLA, Los Angeles, CA 90095-1597, USA

Abstract

The evolution of ceramic breeder pebble bed thermal creep deformation subjected to an external load and a differential thermal stress was studied using a modified discrete numerical code previously developed for the pebble bed thermomechanical evaluation. The rate change of creep deformation was modeled at the particle contact based on a diffusion creep mechanism. Numerical results of strain histories have shown lower values as compared to those of experimentally observed data at 740 °C using an activation energy of 180 kJ/mol. Calculations also show that, at this activation energy level, a particle bed at an elevated temperature of 800 °C may cause too much particle overlapping with a contact radius growth beyond 0.65 radius at a later time, when it is subjected to an external load of 6.3 MPa. Thus, by tracking the stress histories inside a breeder pebble bed the numerical simulation provides an indication of whether the bed may encounter an undesired condition under a typical operating condition.

© 2002 Elsevier Science B.V. All rights reserved.

1. Introduction

Characterization of the elastic and creep properties of ceramic breeder pebble beds under thermomechanical loads is necessary to ensure that the integrity of beds does not become the blanket lifetime limiting factor. Previous experimental results of ceramic breeder Li_4SiO_4 pebble bed thermomechanical tests at temperatures above ~ 650 °C ($\sim 0.5 T_m$) have shown that deformation and/or thermal creep increases as a function of time when the bed is subjected to an externally applied constant pressure [1,2]. These creep rate results have been correlated as a function of temperature and pressure. Contrary to being linearly proportional to stress, which characterizes diffusion creep for a sintered porous form [3], the creep observed in pebble bed configurations shows a stress exponent factor of less than 1. This might indicate that some of the applied stress caused initial particle relocation and bed rearrangement during ther-

mal creep (this is highly possible since the pebble bed was brought to a high temperature state before a uniaxial stress was imposed), and therefore, led to a lower stress exponent factor.

As known, creep deformation depends on many factors including fabrication, material properties, and operating conditions. Depending on the mechanism involved, the creep rate can be a strong function of grain size, porosity fraction, stresses, temperature, and so forth [4–6]. Changes in creep mechanisms are entirely possible with stress relaxation, while it is quite unlikely to deform via the same predominant mechanism at all times during the operation. Despite the complexities involved in the processes, predictions of ceramic breeder pebble bed creep deformations are important and are needed to ensure proper designs and operations. In this current work, experimental observations of creep strains was modeled based on a diffusion creep deformation according to there being a small amount of stress. The objective was to develop an understanding of the effects of applied stress on the deformation characteristics of pebble bed structures at elevated temperatures, while defining operating regimes where pebble bed integrity may be jeopardized. While the present effort does not

^{*} Corresponding author. Tel.: +1-310 206 8815; fax: +1-310 825 1715/2599.

E-mail address: ying@fusion.ucla.edu (A. Ying).

intend to lead to fully developed understanding and modeling of creep behavior, it does point out the areas where data is missing. In addition, although the irradiation effect is not considered in this paper, the goal is to develop a tool for the beginning of life thermomechanics performance prediction for design scoping.

Numerical simulations were used to trace the evolution of contact characteristics and forces as deformation proceeds. A previously developed 3-D discrete numerical thermomechanics code [7] provided initial bed and contact conditions, while a micro-constitutive equation was used to determine the development of creep strain at the contact with time. In the following sections, the simplifications of the basic set of equations describing diffusion creep are outlined and numerical results are presented.

2. Phenomenology of strain deformation

The deformation mechanism of a packed bed at elevated temperatures prior to the occurrence of significant amounts of sintering can involve particle rearrangement, and surface and boundary diffusions. In this paper, the process of elastic plus diffusion deformation is adopted to model the evolution of the bed deformation. Two problems are considered. The first assumes that the source of the deformation originates from the thermal stress caused by the differential thermal expansion, a case in which stress relaxation leads to a reduced strain rate as time progresses. The second involves a bed subjected to an externally applied constant force in which the strain increases as time proceeds yet the strain rate also decreases.

As pressure is applied, it causes localized deformation at the contacts, resulting in work (strain) hardening. This work hardening is reflected through the increase of bed stiffness while the distance between particle decreases. The effect of heating is to provide thermal energy to initiate interparticle mass transport. When heated to temperatures in excess of approximately half of the absolute melting temperature, the pebbles are expected to bond together. Bonding may take place as the neck grows at the point of particle contact. However, this is an undesirable situation for a pebble bed blanket design configuration. Thus, if the model indicates that a sintering process becomes possible because there is too much force exerted on the particles, engineering solutions has to be built in to prevent this. In this sense, the numerical simulation is a useful and economical tool to help identify whether a design would involve an unfavorable thermomechanical state at the earlier stage of the operation.

At high temperatures and low stresses (or before a large deformation has occurred), deformation of materials proceeds by mutually accommodating grain-

boundary sliding and transport of matter. In a deformation based on the Coble creep process, where the transport of matter occurs by grain-boundary diffusion, the strain rate is given as [8],

$$\frac{d\varepsilon}{dt} = \frac{42\delta D_b \Omega \sigma}{\kappa T d^3} = \frac{42\bar{D}_b \sigma}{d^3}, \quad (1)$$

where $\delta D_b (= \delta D_{b0} \exp -(Q/RT)$ where Q is the activation energy and R is gas constant) is grain-boundary diffusion coefficient, $\Omega (= 8.329 \times 10^{-29} \text{ l/m}^3)$ is the atomic volume, κ is the Boltzmanns constant, T is the absolute temperature, d is the particle size, and σ is the effective stress. In a multi-component system, the diffusion coefficient is calculated through a weighted mean of the diffusivities of the component [5].

3. Numerical simulation

The methodology of Svoboda and Riedel [9] of energy rate extremization is applied to solve the problem of a packed bed subject to free and pressure assisted thermal creep deformation. The theory recalls that the sum of the rate of change of the free energy of the system and the rate of energy dissipation has a minimum value with respect to mass flux and surface areas, and that leads to the appropriate governing equations for the mass transport problem on the actual free surface and grain-boundary. The rate of change of particle contact radius (\dot{x}) and instant contact distance (ℓ) at the earlier stage of deformation (or small deformation) are given below (details can be found in [10]):

$$\dot{x} = \frac{4\bar{D}_b(2\gamma_s - \gamma_b)}{xt^2} - \frac{4\bar{D}_b F}{\pi x^3 t}, \quad (2)$$

$$\ell = \frac{1}{x^2} \left[\frac{V_0}{\pi} - \frac{2}{3}(a^3 + b^3) + \frac{x^4}{4} \left(\frac{1}{a} + \frac{1}{b} \right) \right], \quad (3)$$

where γ_s and γ_b are the surface and grain-boundary energies per unit area respectively, \bar{D}_b is defined in Eq. (1), F is the applied force, a and b are particle radii, x is the contact radius at time t , and V_0 is the initial half particle volume of the contact. The second term at the left-hand side of Eq. (3) resembles the Coble's creep deformation.

Few papers have been published in the area of creep deformation with regard to ceramic breeder particularly for a pebble bed configuration. Due to the lack of data, the calculations assume that the potential for matter transport due to the surface and boundary energy is negligible when compared with that caused by the applied and induced stresses. Furthermore, considering that the α -phase of lithiumsilicate has the orthorhombic structure, the pre-exponential constant of the boundary

diffusion coefficient ($\delta D_{b0=1 \times 10^{-10}}$) takes the same value assumed for Mg_2SiO_4 , while an activation energy (Q) of 180 kJ/mol experimentally obtained for Li_4SiO_4 sintered porous material is used [3]. The aforementioned rate change equations are implemented into a previously developed 3-D discrete numerical thermomechanics code to determine the development of creep strain with time. Note that, in this first attempt, particles with spherical shape are used and the shape of the particle remains unchanged during the analysis. During simulation, for each time step, the model takes into account that the contact radius increases as a result of diffusion creep, while the bed hardening is determined by the magnitude of the overlap. The amount of particle relocation is reduced as a result of bed stiffness.

4. Numerical results

Numerical results of strain histories for temperatures of 740 and 800 °C under an applied external stress of 6.3 MPa are shown in Fig. 1 and compared with the experimental results of [1,2]. Here, the strain is defined as the calculated change of the container plate location. Numerically, an equilibrium pebble bed configuration at zero applied pressure is obtained first. A subsequent applied pressure of 6.3 MPa causes particles to shift and rearrange, and produce an initial jump in the strain (this appears different from the actual experimental procedures). The stress-induced thermal creep developed at the particle contacts causes further strain increase. Since

the pressure is maintained through the cause of the evaluation, the creep increases continuously, although the creep rate drops due to a gradual increase of the contact area, which then reduces the deformation rate. It is also noted that experimentally there is a large increase in strain when the temperature increases from 740 to 800 °C. This significant amount of increase in the strain is not captured by the model. Furthermore, the model gives slightly lower than the data obtained at 740 °C. The difference between the calculated and experimental values arises from many factors including model assumption and the lack of physical and material property data. An example of the evolution of particle contacts is illustrated in Fig. 2, which shows how the contact area grows as particles approach each other due to the increase of creep. As creep proceeds, the particle center location is adjusted according to:

$$\Delta(X, Y, Z) = \sum_c^{i=x,y,z} \Delta \ell_c^i, \tag{4}$$

where $\Delta \ell_c$ is the overlapping distance at contact c . As the result of the creep, particle A (as shown in Fig. 2) shifts slightly toward the upper-left corner. The decrease in creep as time proceeds can also be elucidated by the drop of the average stresses exerted on the particles. The average stress exerted on the particles decreases by one order of magnitude as time increases to 2000 min (as shown in Fig. 3). The potential occurrence of sintering or particle bonding caused by the stress as time proceeds is illustrated in Fig. 4, where particles with necks that

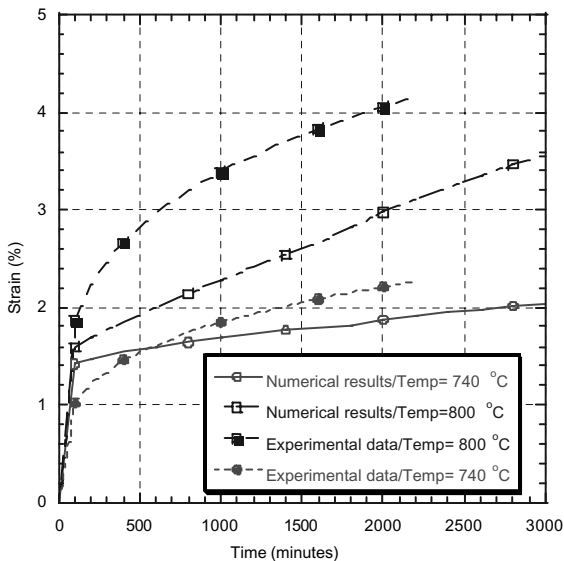


Fig. 1. Comparison of strain as a function of time for two different temperatures. Numerically, initial strain is caused by the particle rearrangement subjected to an external load.

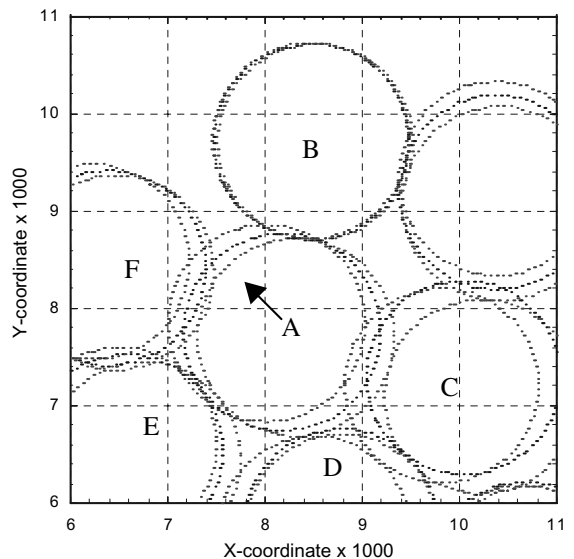


Fig. 2. Particle contact evolutions. As creep proceeds, the contact area increases; total particles simulated: 6760. Particle A shifts slightly toward the upper-left corner due to the compression caused by creep.

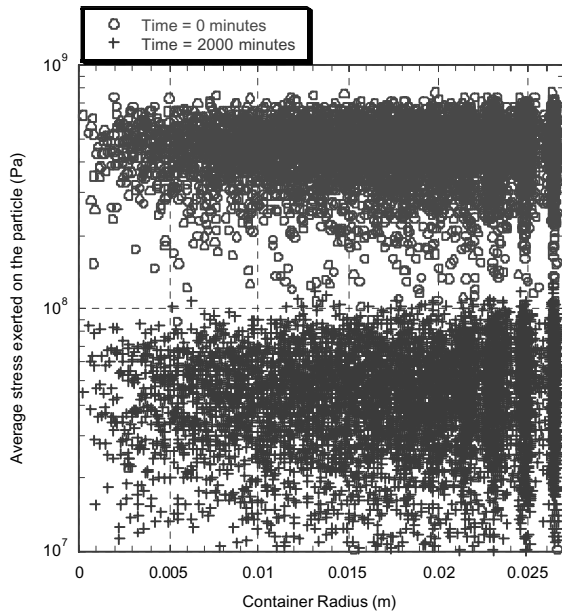


Fig. 3. Average stress exerted on the particles at initial time and at time 2000 min. The average stress drops about one order of magnitude for most of the particles (each symbols represents a particle).

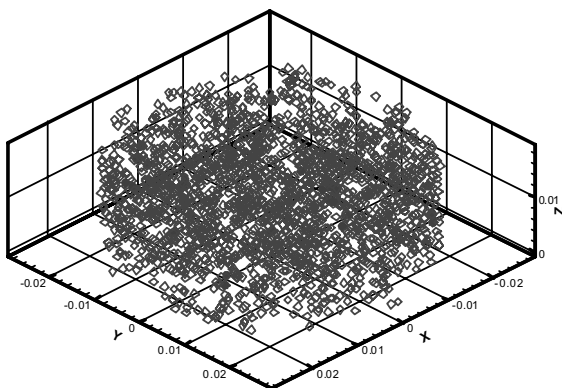


Fig. 4. Particles with contact radius grows beyond 0.65 particle radius at time = 10 min (solid circle) and time = 2000 min (open diamond).

have grown beyond 0.65 particle diameter are plotted at different time intervals. It is surprising to see that about one-third of the particles having a contact radius approaching one particle radius at time = 2000 min, while it is about 1% at time equal to 10 min. The stress evolutions are also simulated for stress generated from a thermally induced breeder-structure interaction. The average stress exerted on the wall as a function of time is shown in Fig. 5. The average stress drops from 18.75

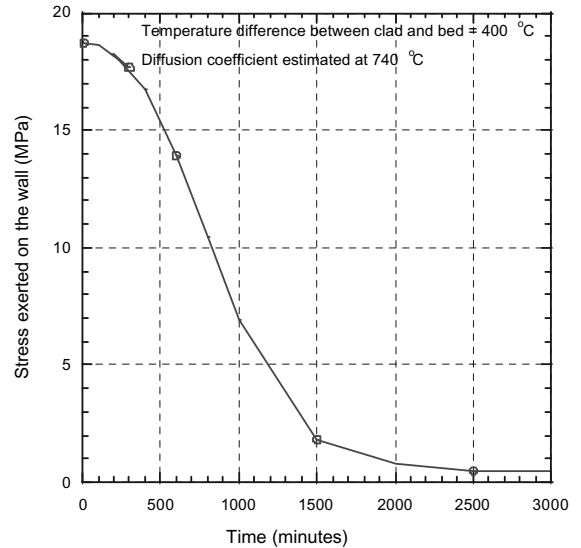


Fig. 5. Average differential thermal stress exerted on the wall as a function of time. Stress is reduced due to thermal creep.

MPa to less than 6.3 MPa at around 1000 min and to less than 1 MPa at around 2000 min after the initiation of creep due to the increase of the contact area caused by creep. This appears to be desirable since the goal is for the stress to be reduced to a significantly lower value at a relatively short period of time after the development of the creep. This should prevent further creep deformation and an undesirable sintering formation.

5. Summary and discussion

In this paper, strain evolutions of a ceramic breeder pebble bed subjected to a thermal differential stress as well as an externally applied stress were numerically studied. The numerical results of strain and strain rates as a function of time based on a diffusion creep mechanism under-predicts what is experimentally observed. However, it is believed that the development of such a tool for simulation is necessary and useful, and will provide an indication as to whether an undesirable sintering condition may or may not occur under the operating conditions by tracking the stress evolution of the bed. It should be stated that the experimental data, phenomenological description, and numerical modeling of the strain response of pebble beds have yet to illuminate what processes are involved. The mechanistic details of pebble bed thermal creep with respect to the contributions from elastic, plastic and diffusion flow, and interfacial sliding, as functions of stress, temperature, and time during creep, should continue to be studied.

Acknowledgements

This work was performed under US Department of Energy Contract DE-FG03-ER52123.

References

- [1] J. Reimann, E. Arbogast, M. Behnke, S. Müller, K. Thomauske, *Fusion Eng. Des.* 49&50 (2000) 643.
- [2] J. Reimann, G. Wörner, Thermal creep of Li_4SiO_4 pebble beds, 21st Symposium on Fusion Technology, Madrid, Spain, 11–16 September 2000.
- [3] H. Zimmermann, Mechanical properties of lithium silicates, in: G.W. Hollenberg, I.J. Hastings (Eds.), *Fabrication and Properties of Lithium Ceramics II*, *Advances in Ceramics*, vol. 27, 1989, p. 161.
- [4] K.C. Goretta, D.S. Applegate, R.B. Poeppel, M.C. Billone, J.L. Routbort, *J. Nucl. Mater.* 148 (1987) 166.
- [5] H.J. Frost, M.F. Ashby, *Deformation-Mechanism Maps*, Pergamon, Oxford, 1982.
- [6] S. Onaka, J.H. Huang, K. Wakashima, T. Mori, *Mech. Mater.* 31 (1999) 717.
- [7] Z. Lu, *Numerical Modeling and Experimental Measurement of the Thermal and Mechanical Properties of Packed Beds*, PhD. thesis, 2000.
- [8] R.L. Coble, *J. Am. Ceramic Soc.* 41 (1958) 55.
- [9] J. Svoboda, H. Riedel, *Acta Metall. Mater.* 43 (1995) 1.
- [10] F. Parhami, R.M. McMeeking, A.C.F. Cocks, Z. Suo, *Mech. Mater.* 31 (1999) 43.